

Coordination Polymer Nanofibers Generated by Microfluidic Synthesis

Josep Puigmartí-Luis,[†] Marta Rubio-Martínez,[‡] Urs Hartfelder,[†] Inhar Imaz,[‡] Daniel MasPOCH,^{*,‡} and Petra S. Dittrich^{*,†}

[†]Department of Chemistry and Applied Biosciences, ETH Zürich, Wolfgang-Pauli-Strasse 10, CH-8093 Zurich, Switzerland

[‡]CIN2(ICN-CSIC), Catalan Institute of Nanotechnology, Esfera UAB, 08193 Bellaterra, Spain

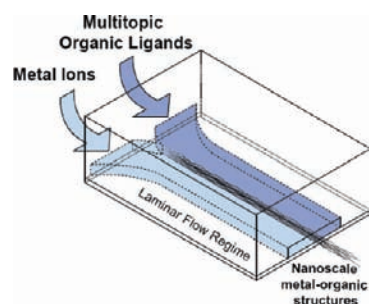
S Supporting Information

ABSTRACT: One-dimensional coordination polymer nanostructures are an emerging class of nanoscale materials with many potential applications. Here, we report the first case of coordination polymer nanofibers assembled using microfluidic technologies. Unlike common synthetic procedures, this approach enables parallel synthesis with an unprecedented level of control over the coordination pathway and facilitates the formation of 1D coordination polymer assemblies at the nanometer length scale. Finally, these nanostructures, which are not easily constructed with traditional methods, can be used for various applications, for example as templates to grow and organize functional inorganic nanoparticles.

In the past decade, huge efforts have been focused on developing new methods for the controlled formation of one-dimensional (1D) nanoscale structures, such as wires, rods, tubes, and fibers, because they play important roles in many applications, including electronics, optics, magnetic devices, drug delivery, and sensors.¹ Nanoscale coordination polymers are an important emerging class of 1D nanomaterials with the intriguing prospect to obtain tailorable morphologies and properties by careful selection of both metal ions and organic ligands.^{2–7} Thus, the design of 1D nanoscale materials containing organic–inorganic components can be particularly interesting for fabricating a new generation of technologically important functional nanomaterials,^{2–5} and for creating novel synthetic biomimetic approaches⁶ and functional gels.⁷ To date, the most common approach for the synthesis of these structures is based on the self-assembly of metal ions and multitopic organic ligands in solution under certain conditions (solvents, temperature, etc.)^{2,3} or employing advanced fabrication methods, such as electrospinning and ultrasound.^{4,5} However, although these approaches are very powerful strategies, more general methods for controlling and guiding the assembly of metal ions and organic molecules to novel 1D coordination polymer structures at the nanometer length scale remain challenging.²

In this regard, lab-on-a-chip approaches have recently attracted tremendous interest for fabricating 1D nanostructures.⁸ Compared to conventional methods, excellent and unique properties appear when scaling-down dimensions inside a microreactor. In particular, the presence of laminar flow makes

Scheme 1. Fabrication of 1D Coordination Polymer Nanostructures Using Laminar Flow in a Microfluidic Platform



microfluidic technologies ideal synthetic and assembly tools due to the superior control over the reaction zone.⁹ Under laminar flow conditions, a stable interface between two reactive streams can be established, while mixing happens exclusively through diffusion. The diffusion and hence the reaction area of different species can be predicted as well as the residence time of species in the microreactor. Therefore the reaction time can be modulated by varying flow rates.¹⁰ While the laminar flow in a microfluidic reactor has been exploited to induce redox and polymerization reactions at the interface of two co-flowing reactant streams to create fibers and wires in the microscale range, we herein demonstrate that microfluidics is as well a straightforward route for controlling the assembly of metal ions and organic building blocks to form 1D coordination polymer nanostructures (Scheme 1). The formation of coordination polymer nanofibers is presented for various compounds: Cu(II) ions and the amino acid aspartate (Asp), Ag(I) ions and the amino acid cysteine (Cys), and Zn(II) ions and the ditopic 4,4'-bipyridine (4,4'-bipy) ligand. The formation of long Cu-Asp nanofibers has recently been shown in a time-consuming bulk reaction,¹¹ which can be massively accelerated in the microdevice to occur within microseconds ($\sim 280 \mu\text{s}$), where the reaction occurs through the entire length of the microchannel (9 mm) at predefined locations and with a preferred orientation. Moreover, Ag(I)-Cys and Zn(II)-4,4'-bipy are novel types of 1D metal-containing nanofibers that cannot be formed in bulk synthetic approaches. Hence, microfluidic-based fabrication can yield nanoscale coordination polymers with

Received: December 2, 2010

Published: March 08, 2011

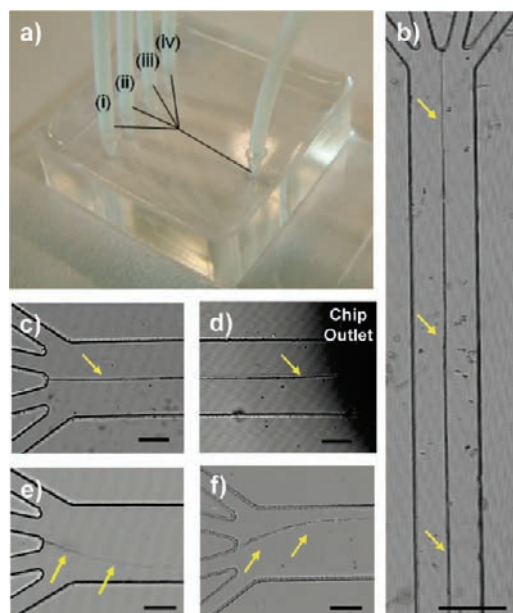


Figure 1. (a) Photograph of the microreactor used in the fabrication of nanoscale coordination polymer fibers. The microreactor contains four inlet channels for supplying the reactants solutions ((ii) and (iii)) and the sheath aqueous flows ((i) and (iv)). (b–f) Optical microscope images of bundles of Cu(II)-Asp nanofibers (yellow arrows) generated inside the chip. (b) Low-magnification optical image of a synthesis performed at [100; 100; 100; 100] (note the broadening of the reaction zone due to diffusion). (c,d) Optical microscope images demonstrating the centered assembly along the main channel length. (e,f) Optical microscope images showing guided assembly when changing the flow rate configuration to [20; 20; 200; 200] and [200; 200; 20; 20], respectively. The scale bar in (b) is 250 μm , and in (c–f) the scale bar is 100 μm .

morphologies and therefore properties that are unequivocally different from those offered by standard synthetic methods.

In a typical synthetic procedure, Cu(II)-Asp nanofibers were initially prepared by injecting two aqueous solutions, one containing $\text{Cu}(\text{NO}_3)_2 \cdot 3\text{H}_2\text{O}$ (1.5 mM) and the second containing L-Asp (1.0 mM) and NaOH (2.5 mM), into a microfluidic platform with four input channels via a syringe pump system at a flow rate of 100 $\mu\text{L}/\text{min}$ (Figure 1a). Both Asp and Cu(II) solutions were injected in the central channels (channels (ii) and (iii) in Figure 1a, respectively), and the formation of Cu(II)-Asp nanofibers through the entire length (9 mm) of the main channel (Figure 1b–d) was accomplished by flowing two aqueous auxiliary streams operating at same flow rate of 100 $\mu\text{L}/\text{min}$ (channels (i) and (iv) in Figure 1a). We define the flow rates (all $\mu\text{L}/\text{min}$) in the different channels by using the following abbreviation: flow (i), Q_i ; flow (ii), Q_{ii} ; flow (iii), Q_{iii} ; and flow (iv), Q_{iv} . Unlike in bulk methods, this methodology enables precisely control of the interface position. Therefore, one can guide the position of the assembly of metal ions and organic ligands along the main channel length by varying the flow rates. When all flow rates are fixed at 100 $\mu\text{L}/\text{min}$, i.e., [100; 100; 100; 100], Cu(II)-Asp nanofibers are assembled in the center of the main channel (Figure 1b–d). However, the formation of these fibers is directed to positions close to the channel walls by changing two flow rates, either Q_i and Q_{ii} or Q_{iii} and Q_{iv} , from 100 $\mu\text{L}/\text{min}$ to 20 $\mu\text{L}/\text{min}$.

Figure 2 shows typical scanning (SEM) and transmission (TEM) electron microscopy images of these structures fabricated

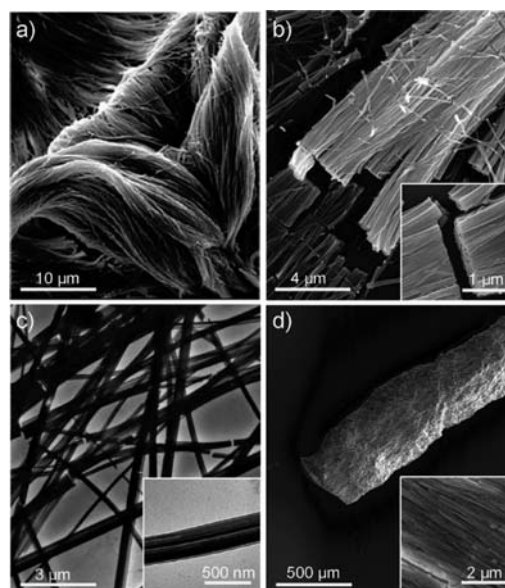


Figure 2. Cu(II)-Asp nanofibers fabricated in the microreactor. (a,b) SEM images of nanofiber bundles synthesized at different concentrations of precursors: (a) 150 mM and (b) 15 mM $\text{Cu}(\text{NO}_3)_2 \cdot 3\text{H}_2\text{O}$. (c) TEM image of these fibers synthesized using a $\text{Cu}(\text{NO}_3)_2 \cdot 3\text{H}_2\text{O}$ concentration of 150 mM. The inset is a high-magnification image of a single nanofiber. (d) SEM images of a Cu(II)-Asp-based xerogel produced in the microreactor and synthesized at a concentration of 1.5 M $\text{Cu}(\text{NO}_3)_2 \cdot 3\text{H}_2\text{O}$. The inset is a high-magnification image, showing the well-aligned nanofibers.

using laminar flow and collected at the end of the main channel. The formation of bundles of well-aligned nanofibers with diameters ranging from 50 to 200 nm can be found. In addition, further characterization by powder X-ray diffraction (PXRD), infrared (IR) spectroscopy, and elemental analysis confirmed the formation of Cu(II)-Asp coordination chains identical to those previously reported.¹¹ The formation of these fibers was also studied by systematically varying the concentrations of both precursor solutions from 1.5 M to 1.5 mM. Under the studied conditions, the formation of fibers was verified, and no significant differences concerning morphology were evidenced (Supporting Information [SI], Figure S2). However, when the microfluidic synthesis was conducted at flow rates [100; 100; 100; 100] and concentrations higher than 1 M, a Cu(II)-Asp based gel was directly eluted from the chip (Figure 2d). A SEM image of the Cu(II)-Asp xerogel directly synthesized in the microreactor shows the good alignment of Cu(II)-Asp nanofibers (inset in Figure 2d; SI, Figure S3). This result confirms that microfluidics is an excellent fabrication technique to control not only the position but also the orientation of metal–organic nanofibers, thus making it possible to envisage the future fabrication of nanofibers with superior performance in comparison with those showing non-oriented geometries, as well as their integration in devices.^{12,13}

The generality and efficacy of the nanofabrication of 1D metal–organic structures using laminar flow in microfluidic devices were studied by generating a second and third type of coordination polymer nanofibers. In the first case, aqueous solutions of $\text{Ag}(\text{NO}_3)$ (1 mM) and Cys (1 mM) were separately injected in channels (ii) and (iii) at a flow rate of 100 $\mu\text{L}/\text{min}$. Again, two aqueous auxiliary streams were injected in channels

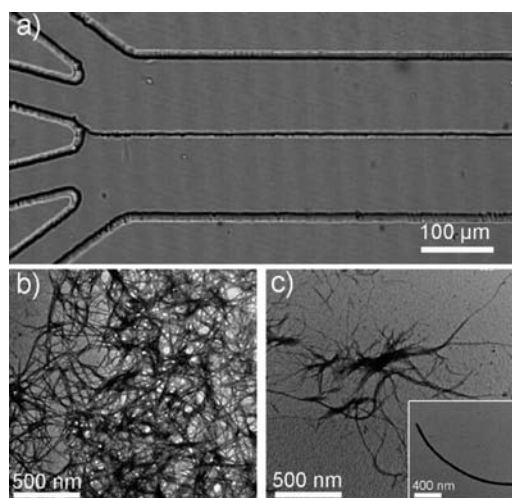


Figure 3. (a) Optical microscope image showing the guided assembly of 1D nanostructure bundles created at the interface between aqueous Ag(I) metal ions and Cys solutions. (b,c) TEM images of the resulting bundles of Ag(I)-Cys (b) and Zn(II)-4,4'-bipy (c) nanofibers just after their elution from the chip. The inset is a high-magnification image of a single Zn(II)-4,4'-bipy nanofiber.

(i) and (iv) at the same flow rate of 100 $\mu\text{L}/\text{min}$. Figure 3a shows the microfluidic guided assembly of 1D Ag(I)-Cys structures at the interface of both reactant flows along the entire length of the main channel. Detailed inspection by TEM of the eluted structures demonstrated them to be constituted of bundles of Ag(I)-Cys nanofibers (Figure 3b; SI, Figure S4). These fibers have diameters between 10 and 50 nm. Similar 1D nanostructures were also obtained when an aqueous solution of Zn(NO_3)₂·6H₂O (100 mM) and another solution containing 4,4'-bipy (100 mM) in ethanol were injected in the microfluidic platform. As shown in Figure 3c, the resulting Zn(II)-4,4'-bipy nanofibers have diameters between 10 and 75 nm (SI, Figure S5). In both cases, the coordinative polymerization of Ag(I) and Zn(II) metal ions through Cys and 4,4'-bipy ligands, respectively, was studied by energy dispersive X-ray (EDX) and IR spectroscopy. First, the EDX spectrum of Ag(I)-Cys fibers corroborates the presence of silver, nitrogen, carbon, and sulfur, whereas zinc, nitrogen, and carbon are observed for the Zn(II)-4,4'-bipy fibers (SI, Figures S6 and S7). The IR spectrum of Ag(I)-Cys fibers confirms the coordination of Cys ligands to the Ag(I) metal ions, as evidenced by the absence of the bands for the S–H group stretching vibration (2546 cm^{-1}), the O–H bending vibration (1419 cm^{-1}), the C–O stretching vibration (1295 cm^{-1}), and the C–O–H combining vibration (1344 cm^{-1} ; SI, Figure S8). Interestingly, this IR spectrum is similar to that recently reported for Ag(I)-Cys small particles, in which a 1D metal–organic structure resulting from the coordination of Ag(I) metal ions through the sulfur atom and weak bonding through the carboxylic group was proposed.¹⁴ Similarly, the IR spectrum of Zn(II)-4,4'-bipy nanofibers includes bands in the range 1639–1333 cm^{-1} associated with the pyridine ring stretching vibrations and bands at 1302 and 812 cm^{-1} , which are attributed to the presence of coordinated nitrate groups (SI, Figure S9).¹⁵

Unlike Cu(II)-Asp nanofibers, the use of conventional methods based on fast mixing of precursor solutions under conditions identical to those used in microfluidic synthesis but with

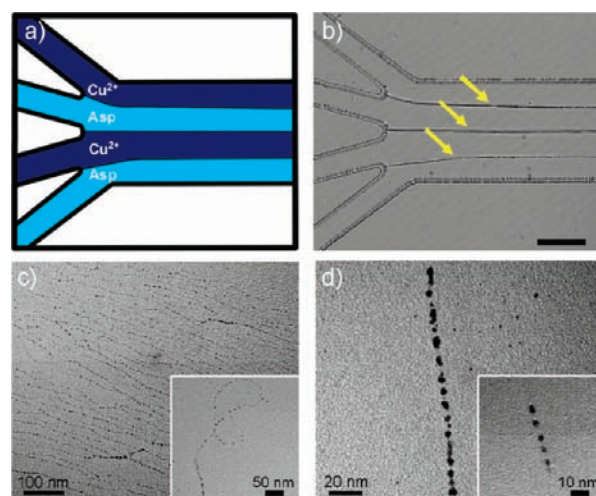


Figure 4. (a) Illustration and (b) optical microscope image of the parallel synthesis of Cu(II)-Asp nanofibers. The scale bar is 100 nm. (c,d) TEM images of the synthesized chain-like superstructures composed of Ag₂S nanoparticles using Ag(I)-Cys nanofibers as templates.

continuous stirring did not lead to the formation of long Ag(I)-Cys and Zn(II)-4,4'-bipy nanofibers. For the Ag(I)-Cys system, the bulk synthesis leads to the formation of membrane-like structures, whereas wider 1D needle-like crystals are formed for the Zn(II)-4,4'-bipy system (SI, Figures S10 and S11). Based on these results, formation of metal–organic polymers using laminar flow in microfluidic platforms seems an effective way for constraining reaction environments and favoring the supramolecular assembly in the form of long 1D nanoscale structures.

An exciting possibility of this fabrication approach using laminar flow is the potential to use the additional channels (i) and (iv) of the microfluidic platform (Figure 1a) to inject reactants and test the capacity of microfluidics to be used as a parallel synthetic methodology for fabricating such 1D metal-containing structures at different pathways inside the main channel. To explore this approach, two aqueous Cu(II) solutions were injected in channels (ii) and (iv), whereas the aqueous Asp solutions were injected in channels (i) and (iii) (Figure 4a). Immediately, as shown in Figure 4b, bundles of Cu(II)-Asp nanofibers were generated at the three interfaces between the four alternating reactant flows. This parallel fabrication should be particularly useful for scaling-up the production and shows promise for synthesizing different types of metal–organic nanostructures at once and even producing metal–organic gels composed of different types of fibers.

All of the data presented thus far point to the ability to form coordination polymer nanofibers and gels using microfluidic synthesis, a capability that could become important for synthesizing unique metal-containing nanostructures with novel functionalities. For example, to test whether these coordination polymer nanofibers can be used as templates for controlling the growth of inorganic nanoparticles, we exposed the Ag(I)-Cys nanofibers collected from the main channel of the microfluidic platform to electron radiation in TEM. Under these conditions, a typical TEM image reveals the formation and organization of semiconductor silver sulfide nanoparticles following the shape of these templates.¹⁶ The resulting nanoparticle superstructures appear in chains composed of individual Ag₂S nanoparticles in

the acanthite phase with diameters between 4 and 9 nm (Figure 4c,d), as confirmed by PXRD¹⁷ and electron diffractions performed via high-resolution TEM and EDX microanalysis (SI, Figures S12–14). Considering that the Ag(I)-Cys nanofibers cannot be easily constructed by traditional techniques or bulk synthetic methods, microfluidic synthesis can be particularly interesting toward the synthesis of new functional 1D inorganic assemblies with important applications in the areas of nanoscale electronics and molecular sensing.¹⁸

In summary, we have presented a new route for a straightforward production of metal-containing nanofibers using microfluidic technologies as a method for guided assembly. We have demonstrated that this methodology enables a fast, better-controlled synthesis and possesses the ability to dictate the formation pathway of the assembled structures simply by varying flow-rate conditions. Considering that many researchers are focused on developing new methods for synthesizing nanoscale coordination polymers,^{2,3} we believe that microfluidics will certainly expand the tools for the fabrication of functional molecular nanoassemblies that are not easily constructed by traditional techniques. Therefore, we believe that this study opens up new opportunities in the design and alignment of (bio)organic–inorganic structures. Ongoing research focuses on the integration of these nanoscale metal–organic materials to other microfabricated structures (e.g., electrodes) for further electrical characterization and applications in the field of nanosensing devices, where anisotropic nanostructures would serve as a convenient building block.

■ ASSOCIATED CONTENT

S Supporting Information. Detailed experimental section, SEM and TEM images and EDX and IR spectra of coordination polymer nanofibers, optical and TEM images of materials obtained in bulk reactions, and PXRD, electron diffraction, and EDX spectra of Ag₂S nanoparticles. This material is available free of charge via the Internet at <http://pubs.acs.org>.

■ AUTHOR INFORMATION

Corresponding Author

dittrich@org.chem.ethz.ch; daniel.masPOCH.icn@uab.es

■ ACKNOWLEDGMENT

This work was funded by the European Research Council under the 7th Framework Programme (ERC Starting Grant, project no. 203428, “ μ -LIPIDS”), VALTEC08-2-003, and MAT-2009-13977-C03. J.P.-L. thanks for the ETH fellowship. D.M. and I. I. thank the Ministerio de Ciencia e Innovación for RyC contracts. M.R.-M. thanks the Institut Català de Nanotecnologia for research fellowships. We thank the Servei de Microscopia of the UAB, the FIRST clean room facilities, and the Electron Microscopy Center of the ETH Zurich for their facilities. Phillip Kuhn and Andreas Cavegn are also acknowledged for their help with figures design.

■ REFERENCES

(1) (a) Schoonbeek, F. S.; van Esch, J. H.; Wegewijs, B.; Rep, D. B. A.; de Haas, M. P.; Klapwijk, T. M.; Kellogg, R. M.; Feringa, B. L. *Angew. Chem. Int. Ed.* **1999**, *38*, 1393–1397. (b) Joachim, C.; Gimzewski, J. K.; Aviram, A. *Nature* **2000**, *408*, 541–548. (c) Huang, Y.; Duan, X. F.; Cui, Y.; Lathon, L. J.; Kim, K. H.; Lieber, C. M. *Science*

2001, *294*, 1313–1317. (d) Ulijn, R. V.; Smith, A. M. *Chem. Soc. Rev.* **2008**, *37*, 664–675. (e) Papapostolou, D.; Howorka, S. *Mol. Biosyst.* **2009**, *5*, 723–732. (f) Amabilino, D. B.; Puigmarti-Luis, J. *Soft Mater.* **2010**, *6*, 1605–1612.

(2) (a) Spokoiny, A. M.; Kim, D.; Sumrein, A.; Mirkin, C. A. *Chem. Soc. Rev.* **2009**, *38*, 1218–1227. (b) Lin, W.; Rieter, W. J.; Taylor, K. M. L. *Angew. Chem. Int. Ed.* **2009**, *48*, 650–658. (c) Hui, J. K.-H.; MacLachlan, M. J. *Coord. Chem. Rev.* **2010**, *254*, 2363–2390. (d) Carné, A.; Carbonell, C.; Imaz, I.; MasPOCH, D. *Chem. Soc. Rev.* **2011**, *40*, 291–305.

(3) (a) Hou, S.; Harrell, C. C.; Trofin, L.; Kohli, P.; Martin, C. R. *J. Am. Chem. Soc.* **2004**, *126*, 5674–5675. (b) Rieter, W. J.; Taylor, K. M. L.; An, H.; Lin, W.; Lin, W. *J. Am. Chem. Soc.* **2006**, *128*, 9024–9025. (c) Jung, S.; Oh, M. *Angew. Chem. Int. Ed.* **2008**, *47*, 2049–2051. (d) Zhang, X.; Chen, Z.-K.; Loh, K. P. *J. Am. Chem. Soc.* **2009**, *131*, 7210–7211.

(4) McDowell, J. J.; Zacharia, N. S.; Puzzo, D.; Manners, I.; Ozin, G. A. *J. Am. Chem. Soc.* **2010**, *132*, 3236–3236.

(5) (a) Chen, Z.; Foster, M. D.; Zhou, W.; Fong, H.; Reneker, D. H.; Resendes, R.; Manners, I. *Macromolecules* **2001**, *34*, 6156–6158. (b) Wang, J.; Dai, L.; Gao, Q.; Wu, P.; Wang, X. *Eur. Polym. J.* **2008**, *44*, 602–607. (c) Zhang, S.; Yang, S.; Lan, J.; Tang, Y.; Xue, Y.; You, J. *J. Am. Chem. Soc.* **2009**, *131*, 1689–1691. (d) Batabyal, S. K.; Peedikakkal, A. M. P.; Ramakrishna, S.; Sow, C. H.; Vittal, J. J. *Macromol. Rapid Commun.* **2009**, *30*, 1356–1361.

(6) Pires, M. M.; Przybyla, D. E.; Chmielewski, J. *Angew. Chem. Int. Ed.* **2009**, *48*, 7813–7817.

(7) (a) Beck, J. B.; Rowan, S. J. *J. Am. Chem. Soc.* **2003**, *125*, 13922–13923. (b) Kawano, S.-i.; Fujita, N.; Shinkai, S. *J. Am. Chem. Soc.* **2004**, *126*, 8592–8593. (c) Kuroiwa, K.; Shibata, T.; Takada, A.; Nemoto, N.; Kimizuka, N. *J. Am. Chem. Soc.* **2004**, *126*, 2016–2021. (d) Hui, J. K.-H.; Yu, Z.; MacLachlan, M. J. *Angew. Chem. Int. Ed.* **2007**, *46*, 7980–7983. (e) Tu, T.; Assenmacher, W.; Peterlik, H.; Weisbarth, R.; Nieger, M.; Dötz, K. H. *Angew. Chem. Int. Ed.* **2007**, *46*, 6368–6371.

(8) (a) Kenis, P. J. A.; Ismagilov, R. F.; Whitesides, G. M. *Science* **1999**, *285*, 83–85. (b) Brazhnik, K. P.; Vreeland, W. N.; Hutchison, J. B.; Kishore, R.; Wells, J.; Helmerson, K.; Locascio, L. E. *Langmuir* **2005**, *21*, 10814–10817. (c) Dittrich, P. S.; Heule, M.; Renaud, P.; Manz, A. *Lab Chip* **2006**, *6*, 488–493. (d) Wang, J.; Bunimovich, Y. L.; Sui, G.; Savvas, S.; Wang, J.; Guo, Y.; Heath, J. R.; Tseng, H.-R. *Chem. Commun.* **2006**, 3075–3084. (e) Gao, Y.; Chen, L. *Lab Chip* **2008**, *8*, 1695–1699. (f) Thangawng, A. L.; Howell, P. B., Jr.; Richards, J. J.; Erickson, J. S.; Ligler, F. S. *Lab Chip* **2009**, *9*, 3126–3130. (g) Puigmarti-Luis, J.; Schaffhauser, D.; Burg, B. R.; Dittrich, P. S. *Adv. Mater.* **2010**, *22*, 2255–2259.

(9) Atencia, J.; Beebe, D. J. *Nature* **2005**, *437*, 648–655.

(10) Ismagilov, R. F.; Stroock, A. D.; Kenis, P. J. A.; Whitesides, G. M.; Stone, H. A. *Appl. Phys. Lett.* **2000**, *76*, 2376–2378.

(11) Imaz, I.; Rubio-Martinez, M.; Saletta, W. J.; Amabilino, D. B.; MasPOCH, D. *J. Am. Chem. Soc.* **2009**, *131*, 18222–18223.

(12) (a) Mor, G. K.; Shankar, K.; Paulose, M.; Varghese, O. K.; Grimes, C. A. *Nano Lett.* **2006**, *6*, 215–218. (b) Tang, Y. B.; Chen, Z. H.; Song, H. S.; Lee, C. S.; Cong, H. T.; Cheng, H. M.; Zhang, W. J.; Bello, I.; Lee, S. T. *Nano Lett.* **2008**, *8*, 4191–4195.

(13) (a) Wittmann, J. C.; Smith, P. *Nature* **1991**, *352*, 414–417. (b) Kuykendall, T.; Pauzauskie, P. J.; Zhang, Y.; Goldberger, J.; Sirbully, D.; Denlinger, J.; Yang, P. *Nature Mater.* **2004**, *3*, 524–528. (c) Zhu, K.; Neale, N. R.; Miedaner, A.; Frank, A. J. *Nano Lett.* **2007**, *7*, 69–74.

(14) Nan, J.; Yan, X.-P. *Chem. Eur. J.* **2010**, *16*, 423–427.

(15) (a) Curtis, N. F.; Curtis, Y. M. *Inorg. Chem.* **1965**, *4*, 804–809. (b) Kim, J.; Lee, U.; Koo, B. K. *Bull. Korean Chem. Soc.* **2006**, *27*, 918–920.

(16) (a) Wang, C.; Zhang, X.; Qian, X.; Wang, W.; Qian, Y. *Mater. Res. Bull.* **1998**, *33*, 1083–1086. (b) Lu, Q.; Gao, F.; Zhao, D. *Angew. Chem. Int. Ed.* **2002**, *41*, 1932–1934.

(17) (a) Yvon, K.; Jeitschko, W.; Parthe, E. *J. Appl. Crystallogr.* **1977**, *10*, 73–74. (b) Aleali, H.; Sarkhosh, L.; Karimzadeh, R.; Mansour, N. *Phys. Status Solidi B* **2011**, *248*, 680–685.

(18) Nie, Z. H.; Petukhova, A.; Kumacheva, E. *Nature Nanotechnol.* **2010**, *5*, 15–25.